Test Application of a High Resolution 3-dimensional Hydrodynamic Model (SUNTANS) to San Francisco Bay

by
Mark Stacey
Rusty Holleman
Edward S. Gross

SAN FRANCISCO ESTUARY INSTITUTE
7770 Pardee Lane, Second floor, Oakland, CA 94621
p: 510-746-7334 (SFEI), f: 510-746-7300, www.sfei.org

This report should be cited as:
Stacey, M., Holleman, R., & Gross, E. S. (2011). Test Applications of High Resolution 3- Dimensional Hydrodynamic Model (SUNTANS) to San Francisco Bay. Contribution No. 638. San Francisco Estuary Institute, Oakland, California.

1. SUNTANS overview

In the past year, we have pursued high-resolution hydrodynamics and transport modeling of specific perimeter habitats as a "proof-of-concept" exercise. The goal was to establish the potential for high-resolution hydrodynamic models to resolve the details of transport in particular locations. The model we applied, SUNTANS is a state-of-the-art hydrodynamic model that allows for the complete solution to the governing equations for fluid motion across a wide range of scales. The model is solved on a triangular mesh (or grid) that can be spatially refined to resolve key features in the domain. The numerics are formulated in a way that permits relatively large timesteps, which facilitates the simulation of real domains much faster than at real-time. For details on the model, we refer to FRINGER REF.

Under funding from the coastal conservancy to Stanford (PIs: Fringer, Koseff and Monismith) and UC-Berkeley (PIs: Stacey and Powell), the application of SUNTANS to San Francisco Bay (SUNTANS-SFBay) is being pursued. In this effort, a full bay model that is extended 50 km out into the Pacific is refined in subembayments to focus on the local dynamics. Specifically, we (UC-Berkeley) have been pursuing a South Bay model, which has high-resolution (~25-50 meter grid size) in South Bay, but coarsely resolves the coastal ocean and Northern San Francisco Bay (grid sizes as large as a few hundred meters). Through that effort, we have been able to focus on the salinity budget for South Bay, which has led us to a comprehensive accounting of freshwater inflows to San Francisco Bay, as well as the inclusion of evaporation at the Bay surface into the numerical scheme. Our experience at the scale of South Bay has established the ability of SUNTANS to successfully simulate the system, as long as the bathymetry and forcing is accurately specified.

In order to successfully apply SUNTANS at the scales and to the locations specified by the perimeter habitats project that we report on here, several additional tools were developed. The details will be described in the next sections, but to summarize: (1) a grid generation tool (funding from both RMP/SFEI and SCC) was developed that allows flexibility without sacrificing robustness; (2) bathymetry data required new interpolations and extrapolations, for which we developed an anisotropic interpolation and explored the use of vegetation type as a surrogate for bed elevation; and (3) model output needed to be compared with direct observations from the study site. The end result is a hydrodynamic and transport model that provides both high-resolution simulation of critical locations and full-bay coverage. This eliminates the need to specify complicated boundary conditions in the interior of the bay and allows forcing to be simplified to an open ocean boundary condition and freshwater forcing.

2. High-resolution modeling of perimeter sites

Through discussions with SFEI and the RMP, three sites were identified as being of particular interest: (1) The Island Pond restoration site, which provides a case study of tidal restoration; (2) Alviso Slough, a mercury "hot spot"; and (3) Hayward Landing, which is also believed to be a contaminant hot spot (Figure 1). For each of these locations, a grid was generated using our new grid generation algorithm and bathymetry data were interpolated onto the grid. At all three sites, the model was successfully run, although the model-data comparison has only focused on Coyote Creek (which is proximal to both the Island Ponds and Alviso Slough locations of interest). In the remainder of this section, we outline the details for the components that make up the high-resolution modeling tool.

2.1 Grid Generation

The grid generating tool (TOM, provided with this report) was used to generate all grids presented in this report (grids also provided with report). The grid generation algorithm is pursued in two steps: First the shoreline must be processed to be compatible with the grid, then

the grid itself is generated. The starting point for the process is an arbitrary resolution, piecewise linear shoreline. A simple preprocessing step creates a topologically consistent polygon with holes from the input. The grid resolution is specified at a number of points and is interpolated over the rest of the domain. The shoreline is preprocessed with an algorithm based on the Delaunay triangulation. It eliminates small inlets that are below the nominal local grid resolution while preserving jetty-like structures. The algorithm computes the Delaunay triangulation of the points along the shoreline, adding Steiner points until the point-Voronoi diagram approximates the edge-Voronoi diagram. Triangles with a diameter smaller than the desired local scale are removed. The shoreline is reconstructed from the remaining triangles and is now ready for grid generation. Compared to simplification algorithms like Douglas-Peucker, this algorithm distinguishes between inlets and jetties. Since it operates in the plane rather than along a polyline it also guarantees that there is enough space to create triangles of the desired scale.

After this processing of the shoreline, the grid generation algorithm uses the Advancing Front method to create the grid throughout the domain, with extensions that ensure orthogonality at every step. The resulting grid is guaranteed to respect the orthogonality condition, and coupled with the simplification algorithm requires very little effort on the part of the user beyond defining the distribution of grid cell sizes.

The grid for the Island Pond site was specified to have approximately 2 meter resolution in the ponds and breaches, expanding to approximately 25 meter resolution near Calaveras Point and hundred of meters through Central and Northern SF Bay. The grid is shown in Figure 2, and illustrates both the full bay coverage (figure 2a), South Bay coverage (figure 2b) and local resolution (figure 2c, 2d). At the finest scale (Figure 2d), it is clear that the breaches and edges of the Island Ponds (where the borrow ditches are) are very highly resolved. The degree of resolution here was chosen in order to capture the local bathymetric variability, which will be discussed in the next section.

The grid for the Alviso Slough site was forced to have similar scales in Central and Northern SF Bay and even into Coyote Creek. The additional requirement in Alviso Slough was that the grid resolution be approximately 4 meters in order to ensure that the Slough was adequately resolved. When generating this grid, we found that the additional resolution required in Alviso Slough was a small perturbation to the Island Pond grid, and we were able to work with essentially the same full-bay grid (figures 3a and 3b, compared to 2a and 2b) and simply refine the grid in Alviso Slough (figures 3c and 3d). In the end, we found that we could simulate the Island Pond and Alviso Slough sites simultaneously with high-resolution in each without the calculations being significantly slower than the grid for either site individually. As such, for the hydrodynamic calculations, the Alviso Slough and Island Pond sites were equivalent (but this is not true for particle tracking).

The final site, Hayward Landing, required a new South Bay grid and the grid generation tool was used to generate a new grid for the entire bay. The resolution requirements for this grid consisted of approximately 2 meters in the vicinity of Hayward Landing, due to the structures present at the site. In order to define the local shoreline, including the presence of jetties and culverts, aerial photography was used in conjunction with NOAA shoreline data. The result is shown in Figure 4, which shows both the entirety of South Bay (Figure 4a) and the local details (Figures 4b and 4c) for the details at the site. At this location, special attention needed to be paid to structures: in Figure 4b a number of jetties are visible; in Figure 4c, both a breakwater and a culvert are evident. For the culvert, we approximated it as a series of obstructions in the

cross-section (the “islands” in Figure 4c), but the parameterization of flow through this structure would require further consideration and analysis.

Comparing the various grids illustrates the power and flexibility of the SUNTANS approach. In all three cases, the full bay grids (Figure 2a and 3a; Hayward Landing not shown) are indistinguishable at the scale of the full domain. Only when we focus on the South Bay can the differences between the site-specific models be seen. In Figure 4a, the grid resolution is clearly focused on the middle of the eastern shoreline of the bay, in the vicinity of Hayward Landing. Comparing this grid to those that focus on the Island Ponds and Alviso Slough (Figures 2b and 3b), we can see that in the far south bay, some details are lost in the Hayward Landing case. Most significantly, the Island Ponds and the Mud Slough complex are not resolved in the Hayward Landing simulations. This is exactly as desired; by not resolving these regions, computational efficiency is gained without compromising model performance at Hayward Landing.

2.2 Bathymetry data and analysis

Once the grids were generated, the next requirement was to specify the depth at each of the grid points. This required both securing and analyzing bathymetry data. For much of South Bay, this effort was already completed as part of the Coastal Conservancy effort. For the high-resolution regions, however, new data sets and analysis tools needed to be explored. In aggregate, the bathymetry data for South Bay came from a number of different sources:

- USGS soundings, 1983, 2005
- USGS lidar, 2005
- Alameda County lidar (after 2006)
- Army Corps sections
- USGS coarse grid (ca 1995)
- Cargill data for Artesian Slough

Outside of South Bay, additional data sources that we have used include:

- NGDC coastal bathymetry
- USGS 10m Delta grid
- NOAA/NOS 30m SF Bay grid
- CSUMB/MBARI side-scan (Golden Gate)

In spite of this variety of data sources, there were still significant gaps in the bathymetry data in the intertidal regions around the Island Ponds, including the Mud Slough complex. In these regions, we developed an approach that used vegetation types from HT Harvey as a surrogate for elevation. Based on typical elevation range for each vegetation type (information also from HT Harvey), we assigned a minimum and maximum elevation to each vegetation type. Using the vegetation map, we defined a contour by the transitions between the vegetation types; the elevation of this contour was constrained by the minimums and maximums for each vegetation type (i.e., it had to fall between the maximum of the two minimums and the minimum of the two maximums). To convert these contours to a surface, we used a function, “surfit”, that obeys the elevation constraints imposed by the vegetation while minimizing the curvature of the surface. Essentially, we defined the smoothest surface possible while remaining consistent with the vegetation maps available.

An additional challenge in the bathymetric data analysis lies in the narrow, sinuous nature of sloughs at the scales being resolved. The bathymetry in these channels is highly anisotropic, with the variability in the along-channel direction being much less than the variability in the

cross-channel direction. As such, a traditional isotropic interpolation of the soundings and sections (USGS, USACE, Cargill) would not accurately reproduce the real bathymetry. Instead, an anisotropic interpolation approach was required, for which we defined the along-channel direction based on the center of the channel (following whatever channel curvature there is, see Figure 3d). Interpolation was done first in the cross-channel direction to define the cross-sectional shape of the channel, then along-channel interpolation was done between sections.

The results of all of these analyses were a collection of bathymetric data sets that together covered the study domain. Datum corrections were then applied and the various data sets were stitched together using GIS methods along with interpolation at boundaries between data sets as needed. The end product is likely the most comprehensive bathymetric data set ever compiled for South San Francisco Bay, with reliable elevation data extending up a number of perimeter sloughs. Excerpts from the bathymetry data are illustrated in Figures 5, 6 and 7. Features of note include the interior of the Island Ponds (Figure 5c), which includes the resolution of the deep borrow ditch that extends around the perimeter of the pond, and the details of the breaches to the Island Ponds (Figure 5d), including even deposition patterns (two high points just inside the breaches) in the interior. The success of the anisotropic interpolation is demonstrated in Figures 6b and 6c, which includes Alviso Slough and makes clear the smooth variation of bathymetry in the along-channel direction. Finally, we note the challenges associated with the Hayward Landing site in Figure 7, where sparse bathymetric data led to highly variable data in the small embayment at the site (Figure 7b) as well as the need to include structures in the bathymetric interpolation (jetties in Figure 7b, culverts in Figure 7c).

2.3 Boundary Forcing

Once the grid and bathymetry are specified, all that remains are the boundary conditions that will drive the SUNTANS calculation. These boundaries fall at the open ocean and at any sources of freshwater to the estuary (Figure 8). At the open ocean boundary, free surface elevation is specified based on tidal harmonic predictions at Point Reyes. We impose a constant salinity at this boundary, which has allowed us (under State Coastal Conservancy funding) to successfully simulate salinity intrusion into South Bay. For all three study sites, we have simulated the period during spring of 2006 (starting from late February) that coincided with both the breaching of the Island Ponds and the collection of data in Coyote Creek (see MacVean 2010 for details).

Freshwater flows were specified throughout the San Francisco Bay and Delta (Figure 8, each blue dot represents a freshwater source). For gauged watersheds, the gauged data was used directly to provide freshwater inflows. For the Delta, DAYFLOW (daily integrated flow entering the Bay) was split between the two artificial channels shown in Figure 8). Finally, flow in ungaged watersheds was estimated based on flows in adjoining gauged watersheds, with a correction based on the ratio of the watershed areas (i.e., we assumed that runoff was proportional to watershed area in extrapolating from a gauged watershed to an ungauged one). Wastewater returns were included from San Jose, Sunnyvale and Palo Alto with data provided by those facilities.

2.4 Observational data sets

As part of funding from the State Coastal Conservancy and the Resources Legacy Fund, data was collected coincidentally with the breaching of the Island Ponds. The details on this data are presented in MacVean 2010 (and MacVean and Stacey, submitted 2011); the study sites are presented in Figure 9, where they are labeled as the West, Center and East stations. At each of these sites, we recorded water level, velocity, salinity and temperature at at least 2 locations in

the water column. In the next section, these timeseries will be compared with the model calculations.

3. *Results of high-resolution modeling*

The observations in Coyote Creek that we will use for model-data comparisons were from March and April 2006. To simulate that period, we spun-up a coarse grid for 6 months in order to get a rough representation of the salinity field, then used the results from that grid as initial conditions for our high-resolution model of the region using the grids and bathymetry shown in Figures 2 and 5. The model output can be captured at any location, and can span the entire two-month simulation period (i.e., 4 spring-neap cycles), and includes tidal stage and velocity and salinity throughout the water column. In the next sections, we focus on the model's performance based on these parameters.

3.1 Water level

All three observational stations have similar variability for tidal stage (or water level). In figure 10, we show the results for the East station; comparisons at the other stations are similar. The period shown includes 5 days in late March, and is representative of the tidal forcing across the two-month period. Comparing the model and observations (Figure 10), we see that the bulk features of the tides are accurately simulated. Specifically, the modeled tidal amplitude and phase are similar to those in the observations, with perhaps the exception of low waters, which are not predicted to be low enough. This agreement is noteworthy, since the tidal boundary condition is imposed 50 km out in the coastal ocean and the tidal wave is dispersed, dissipated and then amplified as it makes its way through Central and South San Francisco Bay.

3.2 Tidal velocities

Again comparing conditions at the East station, Figure 11 shows velocities at two elevations in the water column (at 150 cm and 50 cm above the bed). This is a more difficult prediction than tidal stage since local friction and bathymetry can alter the velocities more directly than they can alter tidal stage. Nonetheless, at 150 cm above the bed, both components of velocity (along-channel and cross-channel; Figures 11a and 11b) are in good agreement with the observations, particularly in terms of the temporal phasing. The model's amplitude does exceed the observed (also reflected in the along-channel component at 50 cm above bed, Figure 11c), which is likely a result of inaccurate bathymetry on the mudflats at the head of Mud Slough, which leads to an inaccurate tidal prism at the Coyote Creek sites. A more serious discrepancy between model and data is seen in the cross-channel component at 50 cm above the bed (Figure 11d) where, even though the magnitude and timing of the flows is reasonably accurate, the predictions are nearly exactly out of phase with the observations. Because this is the cross-channel component, it is very sensitive to local bathymetric contours and, at this station, the observations were very close to the channel-mudflat transition. Subtle errors in the orientation of the bathymetric contours are likely responsible for this model-data mismatch.

3.3 Salinity

The salinity distribution along the axis of an estuary or, in this case, along Coyote Creek, is a result of transport by the tidal velocities (shown in Figure 11) and their interaction with turbulent mixing. Frequently, in order to accurately reflect salinity intrusion, calibration of internal dynamics, particularly bed friction or mixing parameterizations, must be pursued. In this case, because this was a proof-of-concept exercise, we did calibrate the salinity field, but instead simply did a careful accounting of freshwater sources and then let the SUNTANS calculations take care of the internal dynamics. The results are shown in Figures 12, 13 and 14, and the model-data comparison is quite encouraging.

First, in Figure 12, we compare the modeled and observed salinity time series at the East station. First, we note that the average value of the salinity (across the time period shown, e.g.) is well-reproduced by the model. This indicates that the larger-scale (and long timescale) transport, which is bringing salt into Coyote Creek from South Bay, is being accurately modeled. At a more refined level, the tidal variability is also reproduced by the model, which is capturing both the magnitude and phasing of the tidal fluctuations in salinity. The only feature that is not reproduced in the model is the abrupt drop in salinity during each ebb tide; in the model the decrease in salinity is more gradual, which probably reflects errors in the upstream bathymetry that produce increased mixing of the salinity field.

In Figure 13, we examine a similar comparison but at the West station. Here again, both the average salinity and the tidal variations are accurately simulated by the model. At this station, even the ebb periods are more accurately reproduced, due to the fact that the observations tend to show a less abrupt drop in salinity during the ebbs than is seen at the East station. Further, we note that at the West station, the salinity measurements were at the surface and the bottom, so the model's ability to accurately reproduce both timeseries indicates that it is able to effectively characterize vertical stratification, at least in bulk terms, which represents an even more refined test of model performance.

In addition to vertical gradients, we examined the model's ability to reproduce lateral gradients in Figure 14. We note here that observations of lateral gradients were actually made during the fall when the average salinity was much higher. Our comparisons here focus instead on the qualitative variability of the lateral difference in salinity between the channel and breach stations (shown in Figure 15). The modeled and observed time series of salinity at the channel center and breach (Figures 14a and 14b) both show the same general features: the channel station shows tidal variability like that seen in Figures 12 and 13 while the breach station shows an extended period of constant salinity during the ebb tides. This period of constant salinity results from mixing in the interior of the ponds and the model-observation agreement on this point reinforces the fact that we are accurately capturing the detailed dynamics in the pond interiors. Estimates of the lateral salinity gradient (Figures 14c and 14d) also show the same qualitative form between the model and observations, and even similar magnitude, although the details of the timing of some features are shifted.

Taken together, we believe the SUNTANS model has been demonstrated to have been successful at capturing hydrodynamics and transport at the scale of small perimeter habitats. The accuracy with which the salinity field is reproduced is a testament to the quality of the bathymetry data and the ability of SUNTANS to accurately resolve the internal dynamics of complex estuarine flows. While only qualitative comparisons are shown, the fact that the basic features of both the vertical and lateral salinity gradients are reproduced leads to additional confidence in the approach.

3.4 Data output

The SUNTANS model produces three dimensional fields of velocity and salinity that vary tidally. In figure 15, data output locations are documented, including NOAA gauges (Figure 15c), USGS Polaris cruises (Figure 15b) and the Island Pond observations (Figure 15a). Additional results have been output from the key locations noted in Figure 1, specifically the Dumbarton Narrows and Calaveras Point.

4. Discussion of SUNTANS effort

In summary, we believe that we have successfully established the ability of SUNTANS to effectively simulate the local dynamics at perimeter sites of interest. As a necessary part of this

effort, we have developed a new bathymetric data set for South Bay that includes small-scale perimeter habitats as well as a new grid generation tool that can produce flexible, robust grids for numerical models. The resulting grids and bathymetric data sets will be provided to SFEI. Using these data sets, SUNTANS was successfully run for all three study sites, and we evaluated its performance in Coyote Creek, adjacent to both the Island Pond and Alviso Slough sites of interest.

Although the calibration to conditions in Coyote Creek is not complete, we believe the agreement with the observed salinities demonstrates that the fundamental processes are being simulated correctly. If SUNTANS modeling efforts were to continue at these sites, we would recommend a few specific steps be pursued:

1. Adjust tidal prism at mud slough (Island Pond and Alviso Slough sites). This is the key uncertainty that is likely creating the model-data discrepancy in Coyote Creek.
2. Evaluate and collect bathymetry data at the Hayward Landing site. At this point, the available data is quite limited.
3. Collect basic hydrodynamic observations at Hayward Landing, including tidal stage, velocity and salinity.
4. Calibration of parameterization of structures at the Hayward Landing site. The presence of culverts and jetties may require additional parameterization and careful calibration, since these effects are not necessarily captured in the internal dynamics of SUNTANS.

Although we believe that we have established the ability of SUNTANS-SFBay to effectively simulate the dynamics in perimeter habitats, depending on the questions being raised, there may be other approaches that are more appropriate. A SUNTANS-like approach (i.e., high-resolution hydrodynamic and transport simulation) will be useful when local details need to be known, such as patterns of sediment resuspension or the time trajectory of particles emerging from a particular watershed. More aggregated analyses, however, may be appropriate in many cases, particularly when the constituents themselves require complicated modeling.

Regardless of the choice of modeling approach, high-resolution modeling like that presented here may have an important role to play. Specifically, high-resolution models can be used to parameterize unresolved processes in coarse model, or provide forcing and boundary condition information to nested coarse models. At a minimum, high-resolution models can be used to verify the performance of coarse models at the sites of interest. In preparation for those activities, we will provide stage, velocity and salinity data from the simulated period (March-April 2006) at several key locations in the Bay with this report. These sites will include the Dumbarton narrows, Calaveras Point and adjacent to the Island Ponds. Additional data from locations noted in Figure 15 can also be provided as needed.

5. Recommendations

As we have noted, this low-level effort ($35,000) was intended as a proof-of-concept exercise to establish the ability of SUNTANS to resolve local-scale dynamics. The next steps in RMP modeling efforts will necessarily be shaped by the questions being considered. The most important step in this process, therefore, is to define clearly and completely the questions that need to be analyzed, including the critical spatial and temporal scales in addition to the contaminants of interest. Once those questions are framed, then the appropriate mix of modeling studies can be formulated. For example, if the decision is made to analyze where mercury in the sediments of Alviso Slough may deposit following a restoration effort, then a highly detailed transport model is necessary. It is important to recognize, however, that the analysis of a question like this with a model like SUNTANS is resource-heavy (both time and

money) and may be prohibitive. The use of simplified modeling approaches (multi-box models, e.g.) provide a less costly alternative, but the uncertainties inherent in the transport predicted by those models means that their results need to be analyzed carefully, and explicit treatment of uncertainties (through Monte Carlo analysis, scenario analysis or formal error propagation) is critical. In pursuing a box model, high-resolution models could be used to constrain some of the unknown parameters, such as exchange rates between boxes, and could also be used to validate the aggregated results of the box model (e.g., bulk fluxes exiting Alviso Slough).

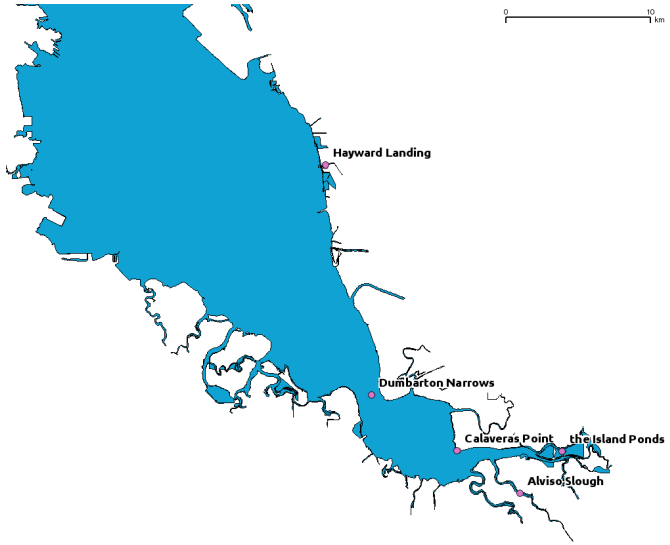

Figure 1: Study location map, identifying the three study sites (Island Ponds, Alviso Slough and Hayward Landing) as well as the Dumbarton Narrows and Calaveras Point, two locations relevant to model setup.

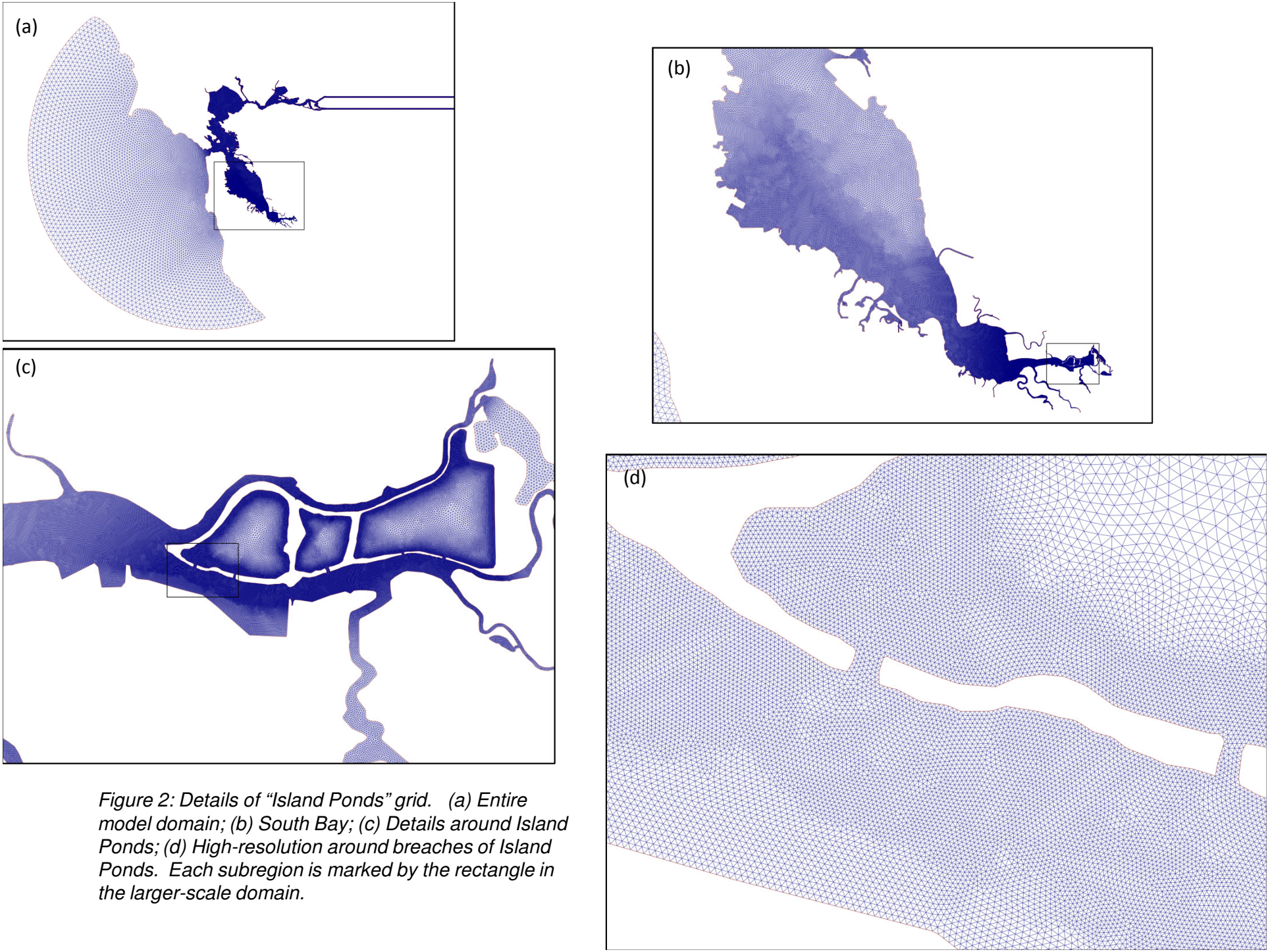

Figure 2: Details of "Island Ponds" grid. (a) Entire model domain; (b) South Bay; (c) Details around Island Ponds; (d) High-resolution around breaches of Island Ponds. Each subregion is marked by the rectangle in the larger-scale domain.

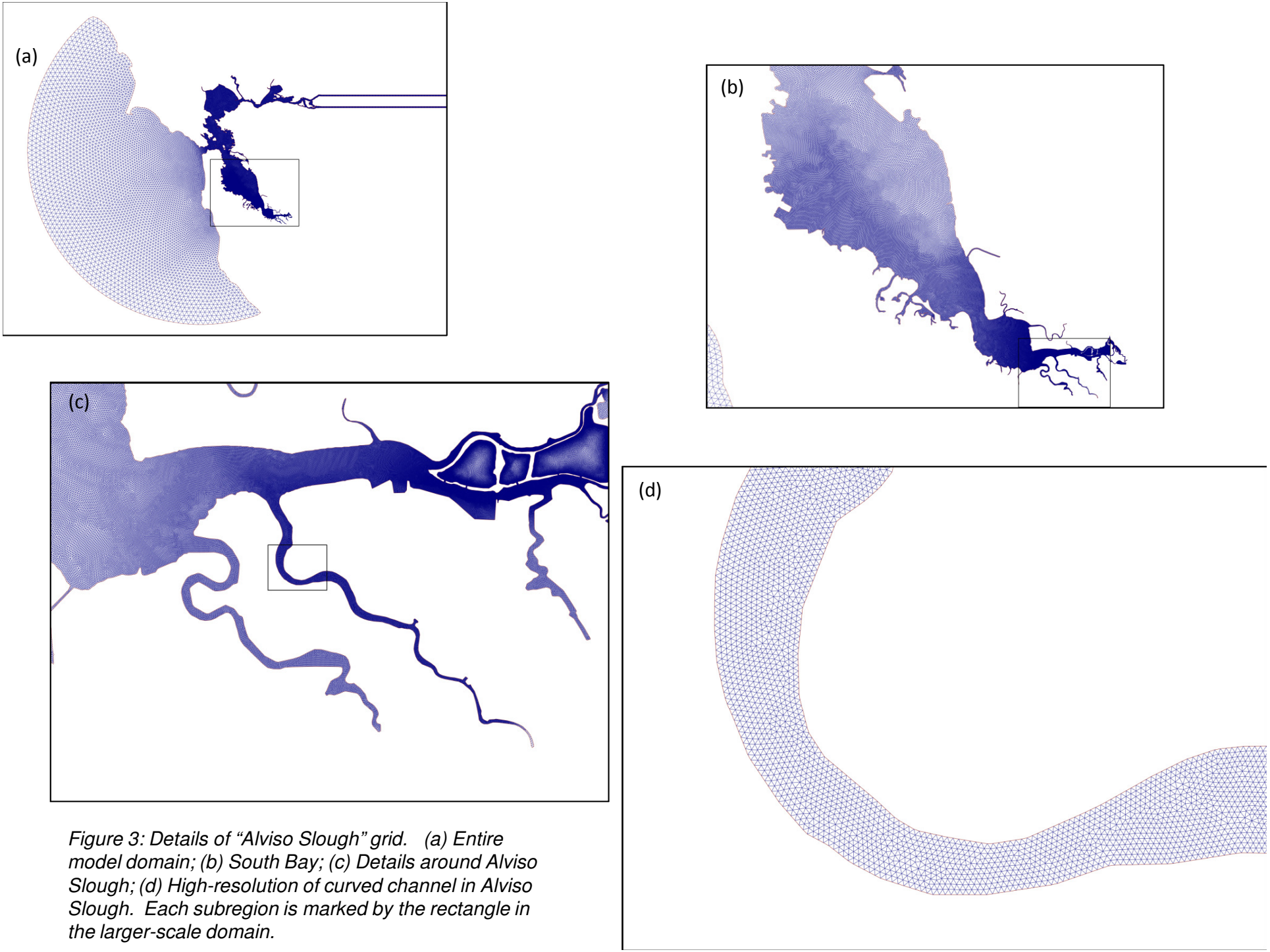

Figure 3: Details of "Alviso Slough" grid. (a) Entire model domain; (b) South Bay; (c) Details around Alviso Slough; (d) High-resolution of curved channel in Alviso Slough. Each subregion is marked by the rectangle in the larger-scale domain.

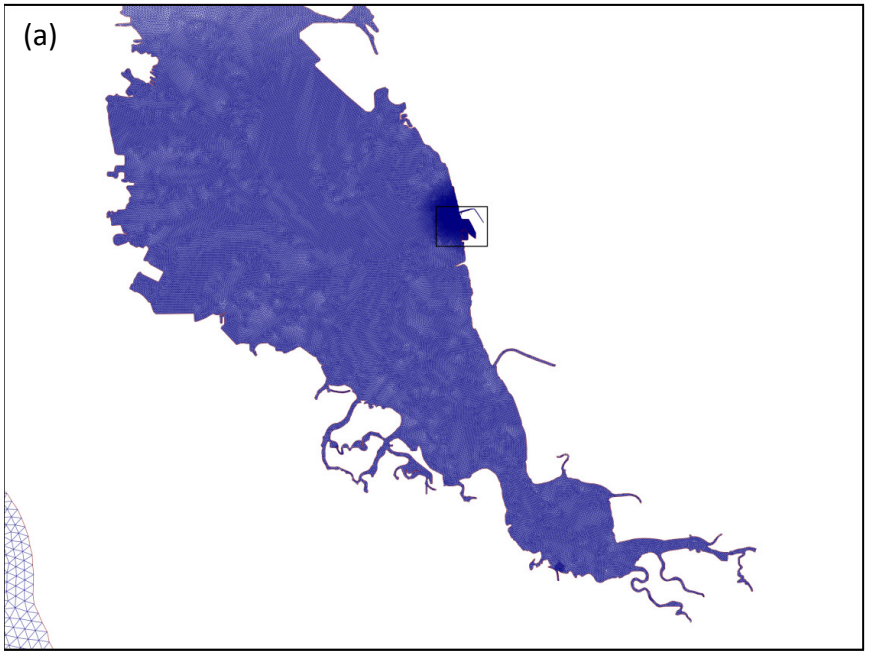

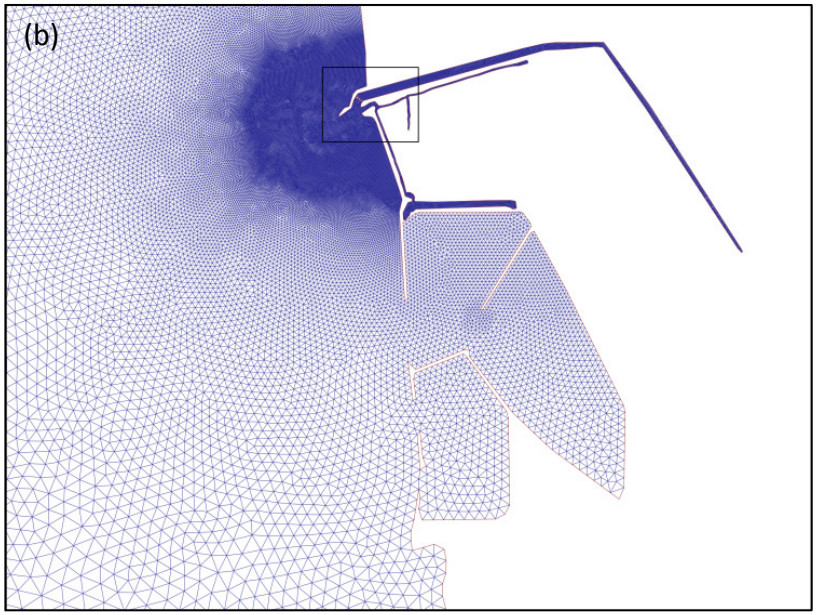

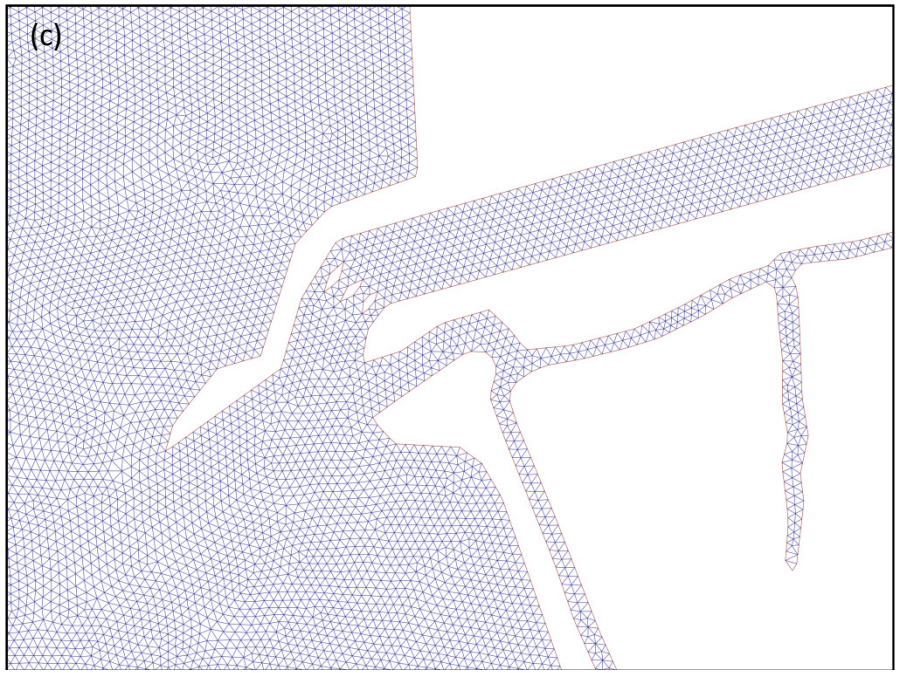

Figure 4: Details of "Hayward Landing" grid. Full Domain is the same as in Figures 2a and 3a. (a) South Bay; (b) Details around Hayward Landing, including jetties; (c) High-resolution of channel mouth at Hayward Landing, note three "islands" to represent culvert. Each subregion is marked by the rectangle in the larger-scale domain.

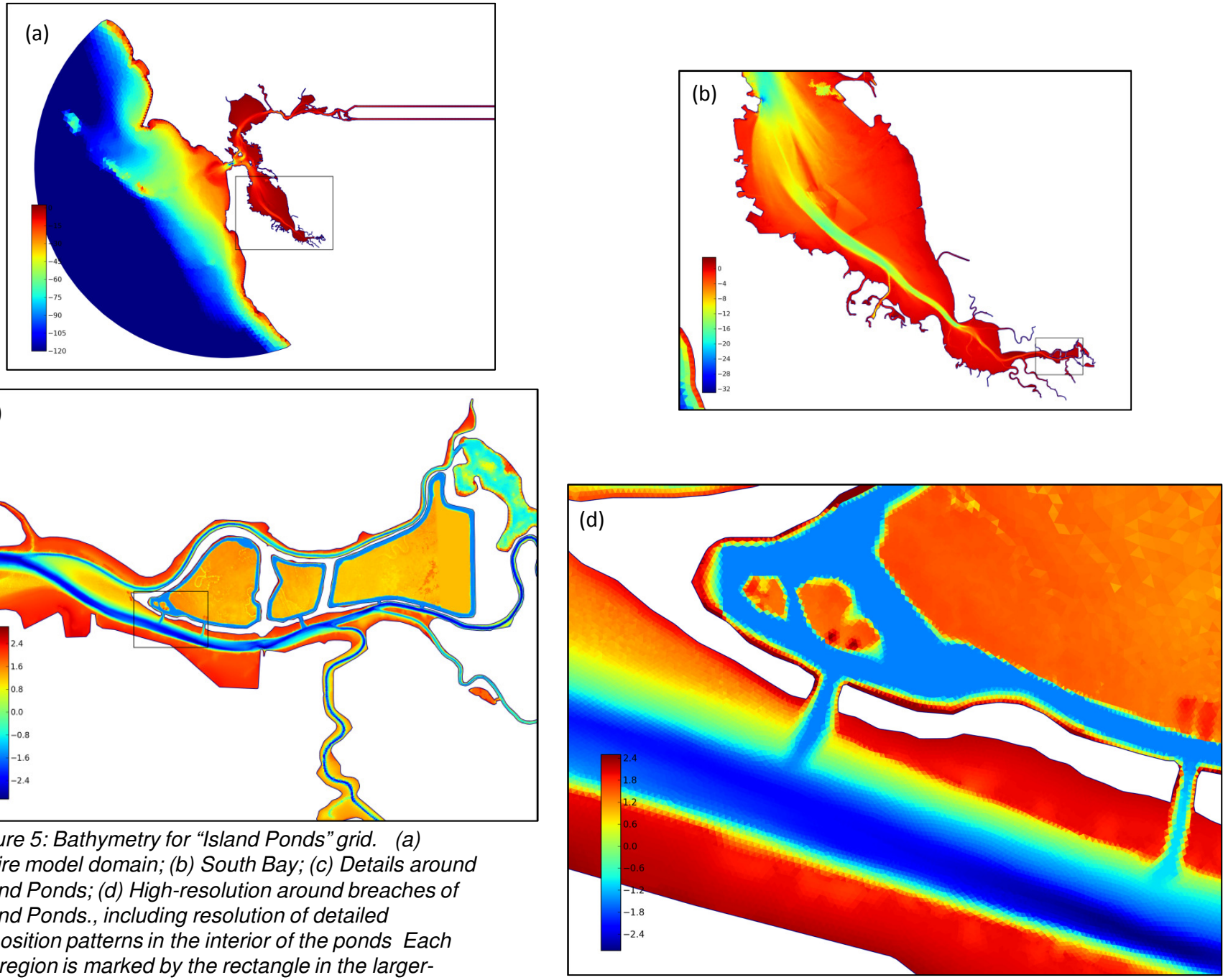

Figure 5: Bathymetry for "Island Ponds" grid. (a) Entire model domain; (b) South Bay; (c) Details around Island Ponds; (d) High-resolution around breaches of Island Ponds., including resolution of detailed deposition patterns in the interior of the ponds Each subregion is marked by the rectangle in the larger-scale domain.

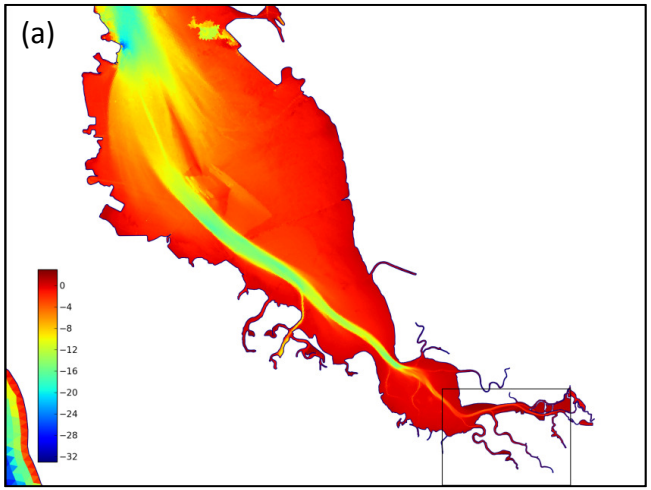

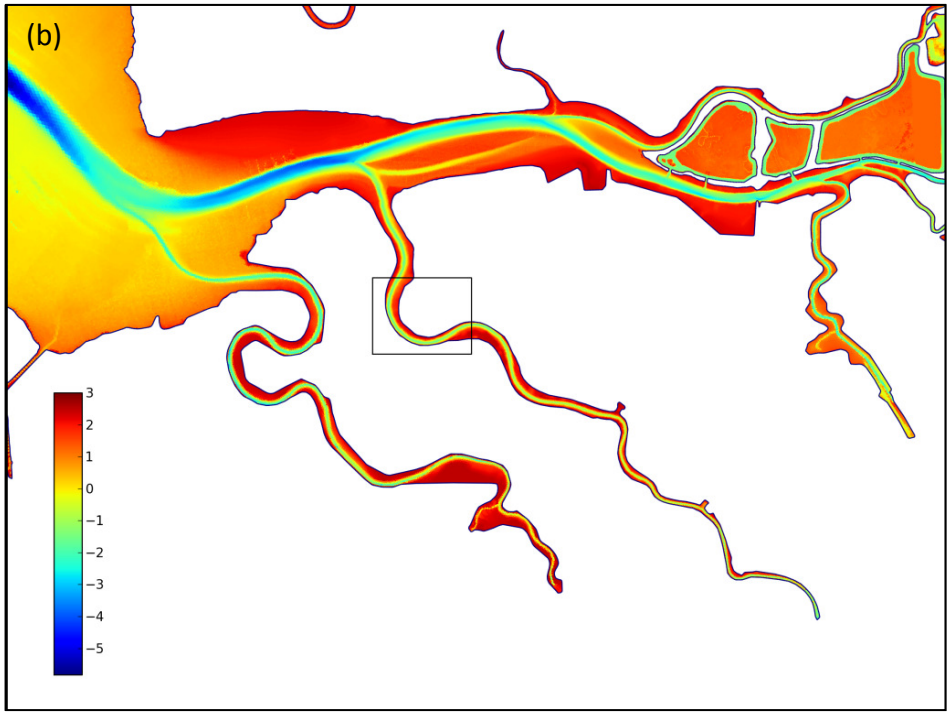

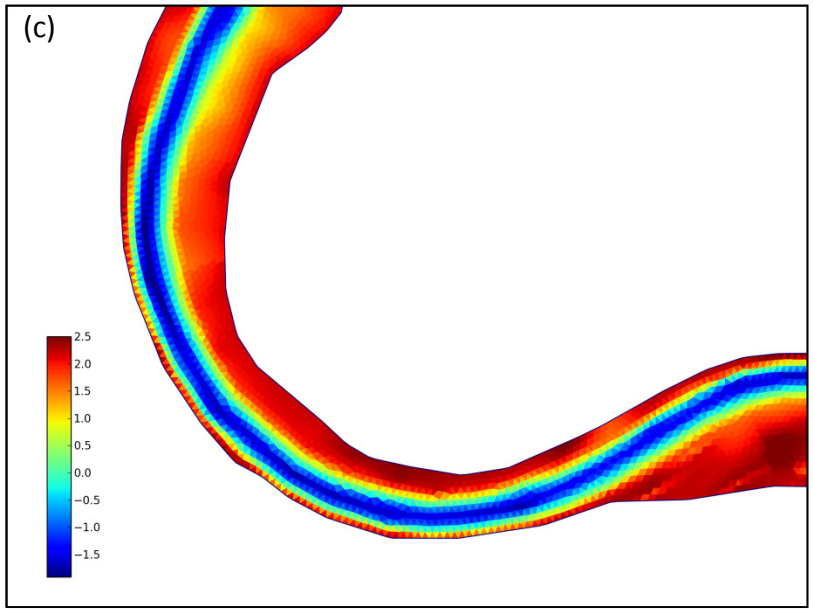

Figure 6: Bathymetry for "Alviso Slough" grid. (a) South Bay; (d) Details in region surrounding Alviso Slough; (c) High-resolution of curved channel in Alviso Slough. Each subregion is marked by the rectangle in the larger-scale domain.

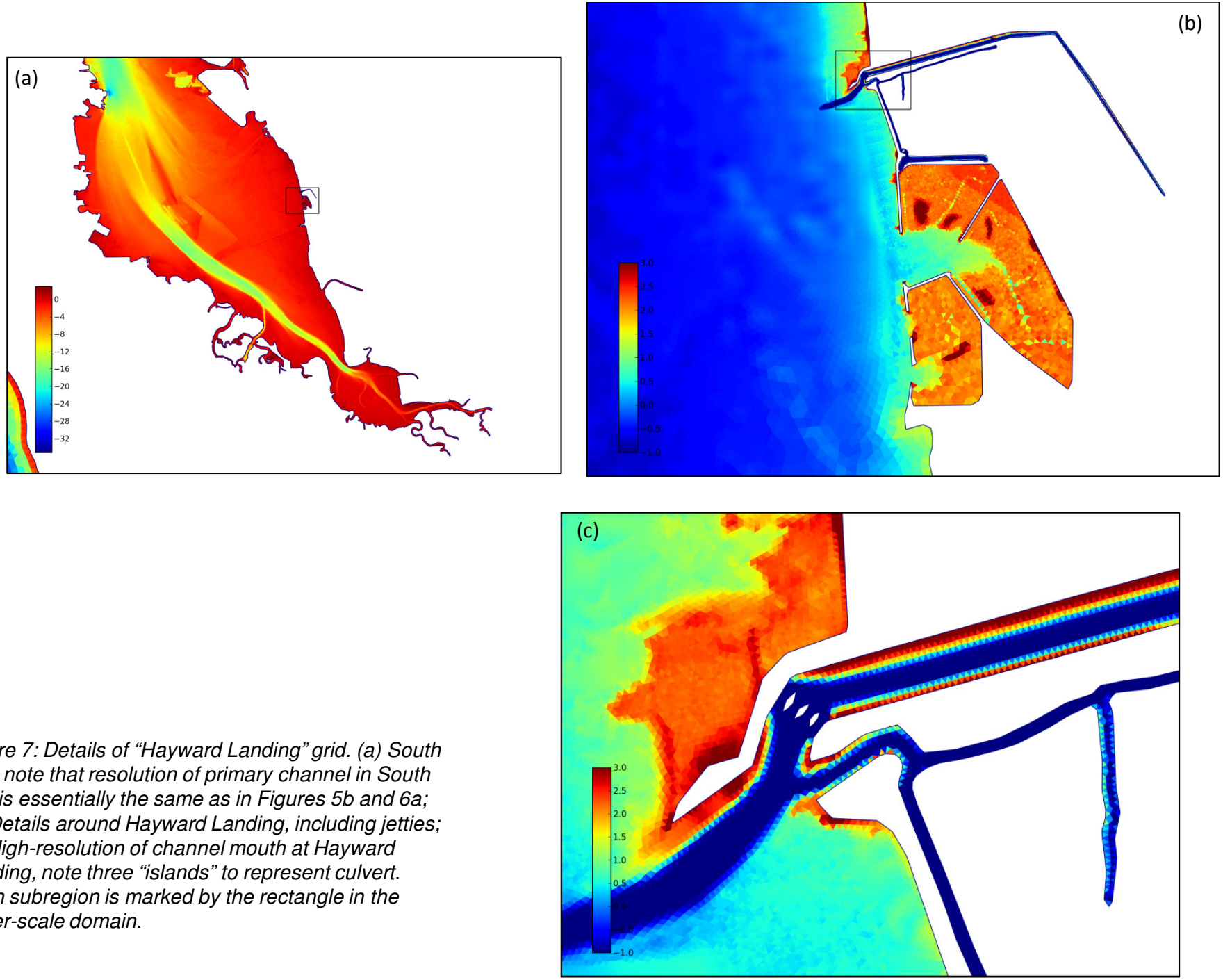

Figure 7: Details of "Hayward Landing" grid. (a) South Bay; note that resolution of primary channel in South Bay is essentially the same as in Figures 5b and 6a; (b) Details around Hayward Landing, including jetties; (c) High-resolution of channel mouth at Hayward Landing, note three "islands" to represent culvert. Each subregion is marked by the rectangle in the larger-scale domain.

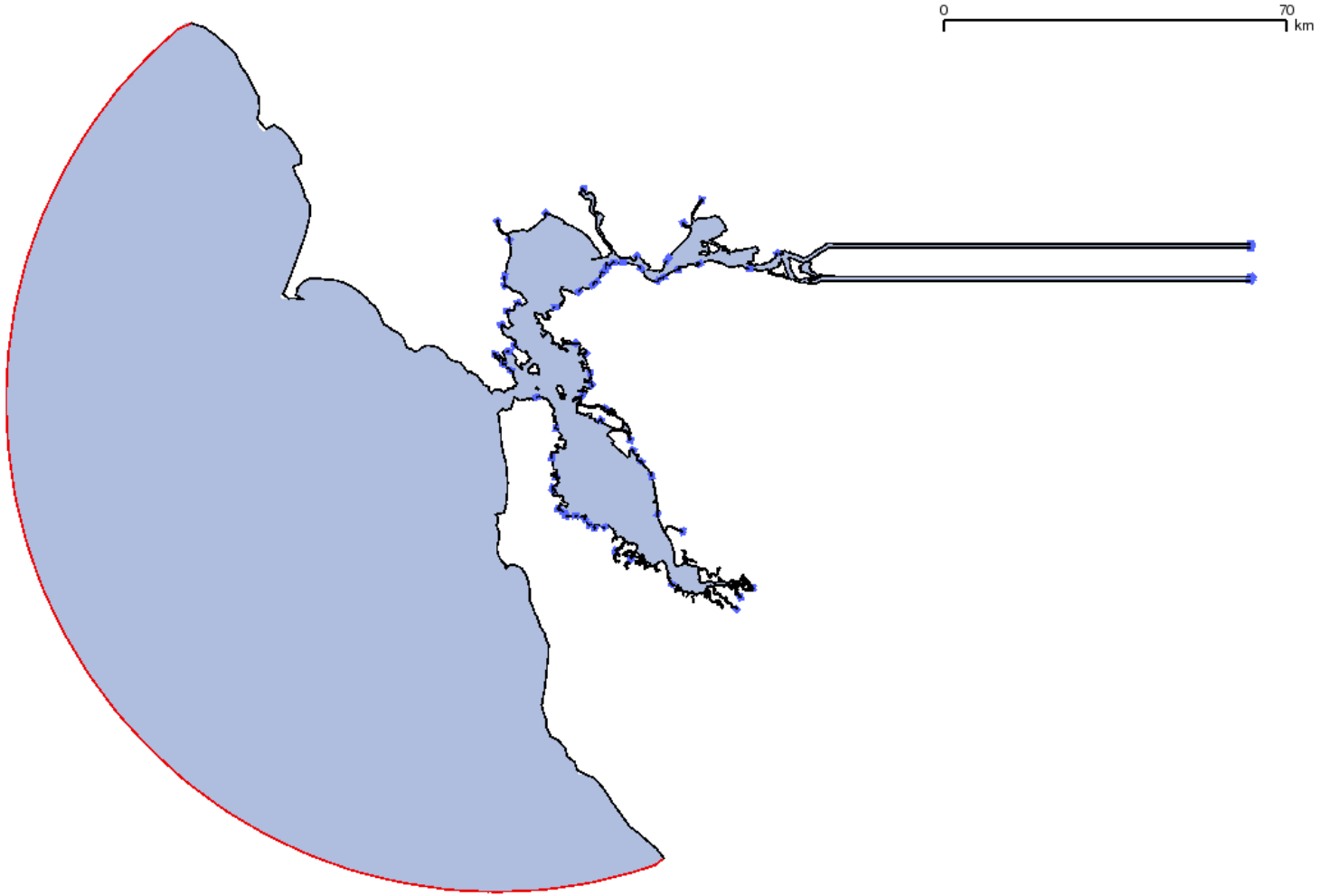

Figure 8: Model domain showing boundary forcing locations. Red boundary represents open ocean boundary, which is forced with Point Reyes tidal constituents. Each blue dot represents a freshwater source, including major and minor rivers, small ungaged watersheds and wastewater returns.

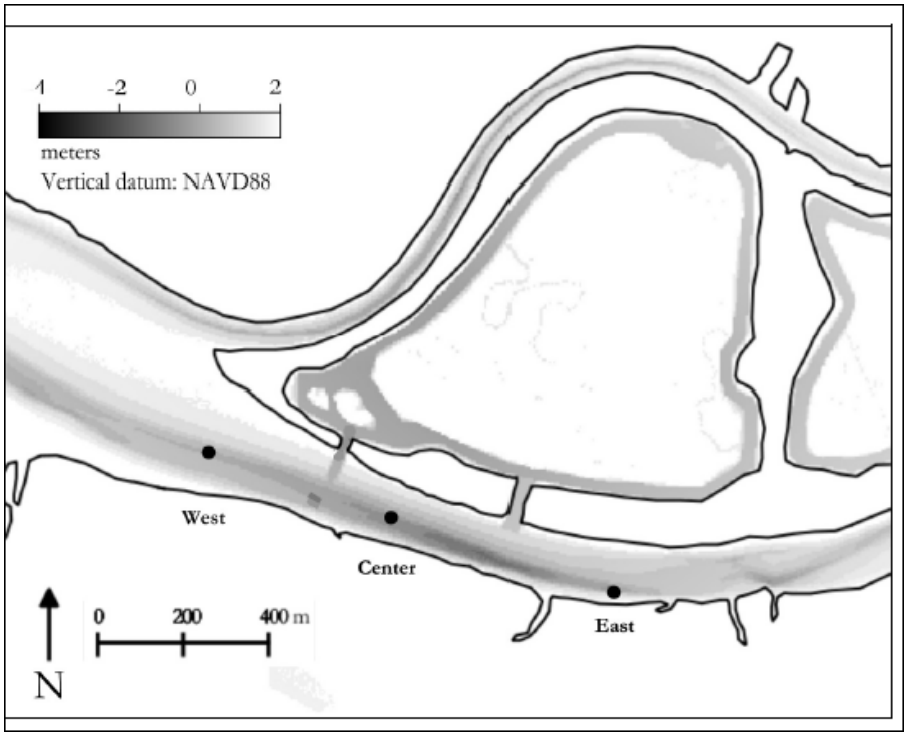

Figure 9: Observation sites for model-data comparison. Data was collected at "West", "Center" and "East" stations for a two month period immediately following the breaching of the Island Ponds. Data included point velocity measurements (using acoustic Doppler velocimeters or ADVs) at Center and East and a velocity profile (using an acoustic Doppler current profiler or ADCP) at West. Additional observations consisted of timeseries of salinity, temperature, pressure and optical backscatter at all three stations.

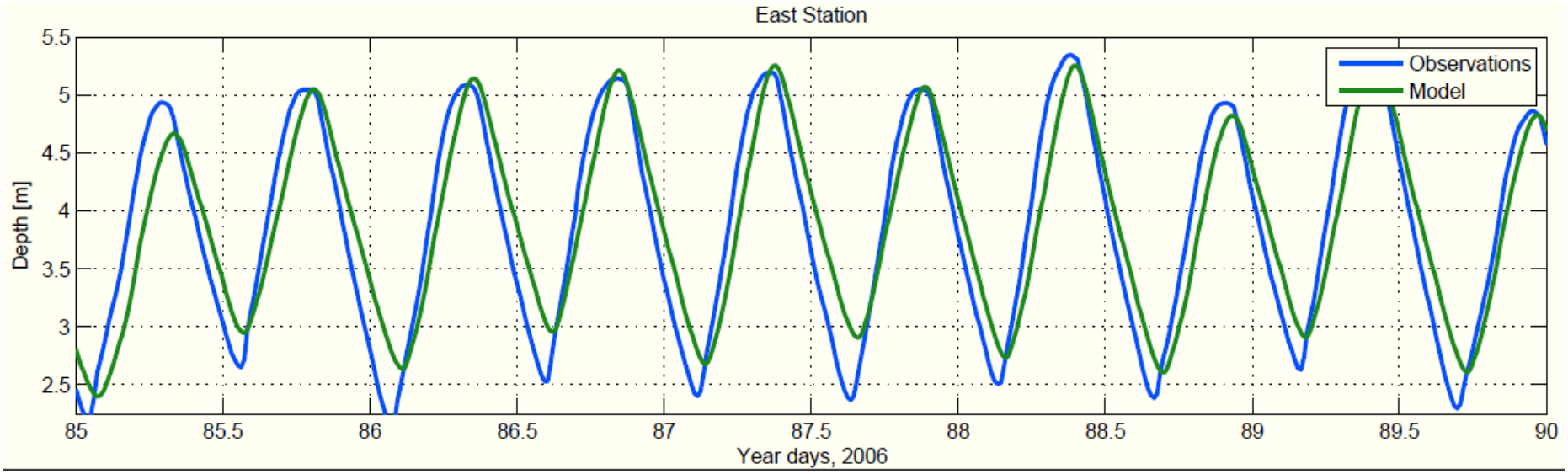

Figure 10: Comparison of modeled and predicted depth at the "East" station for 5-day period in March 2006 (this period is excerpted from entire two-month period for presentation purposes). In general, the magnitude and phasing of the tides are quite well-reproduced (remembering that the tidal boundary condition is imposed 50 km out in the coastal ocean). High tides are accurately modeled, but the low tides are underestimated (i.e., not low enough), which may reflect an inaccuracy in the bathymetry upstream of the study site.

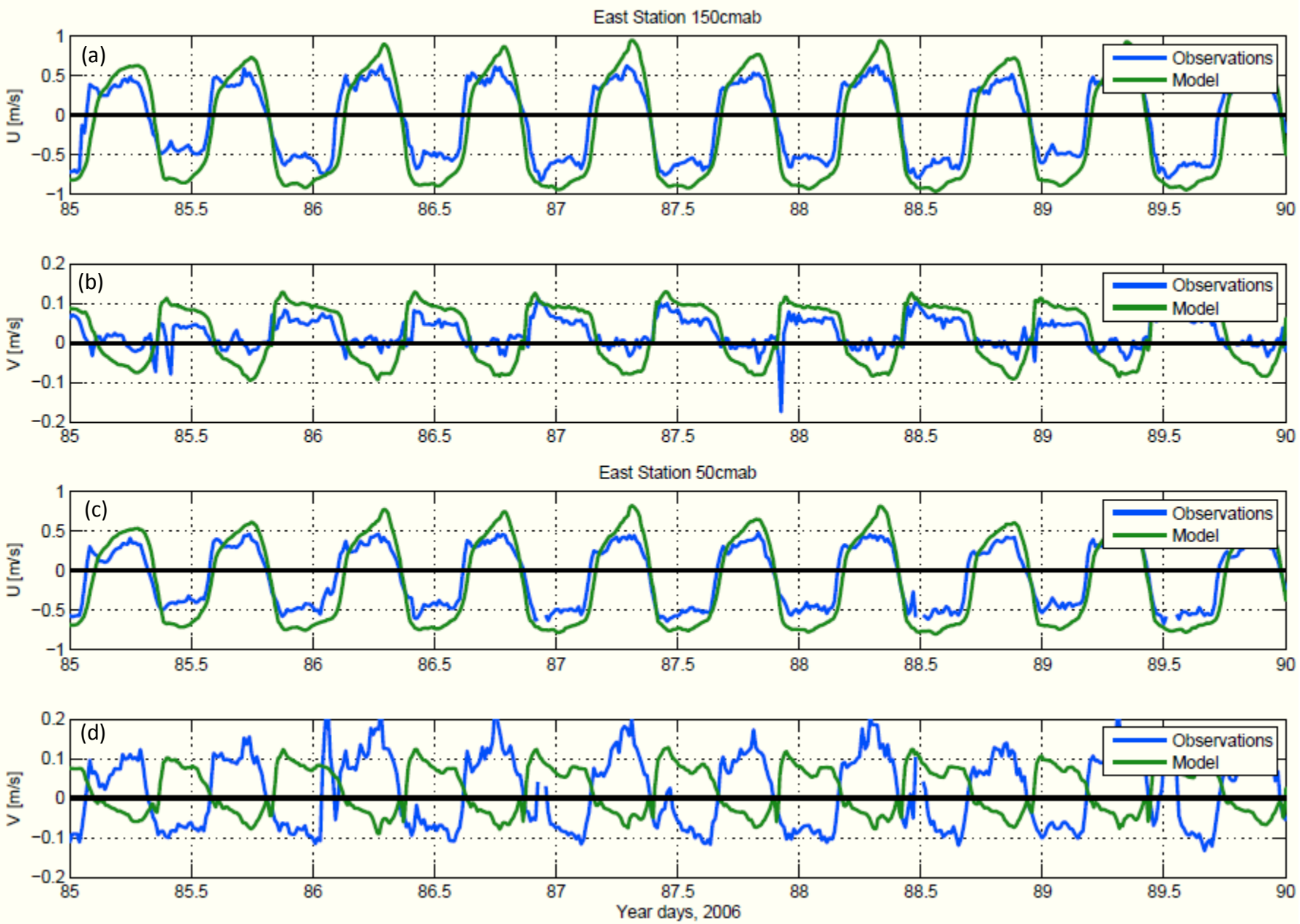

Figure 11: Comparison of modeled and predicted velocity at the "East" station . (a) and (c) represent the along-channel velocities at heights of 150 and 50 cm above the bed, respectively. Cross-channel components are shown in (b) and (d). All components match observations quite well in terms of magnitude and phase, with the exception being the cross-channel component at 50 cm (d), which is nearly exactly out of phase, most likely reflecting local bathymetric contours.

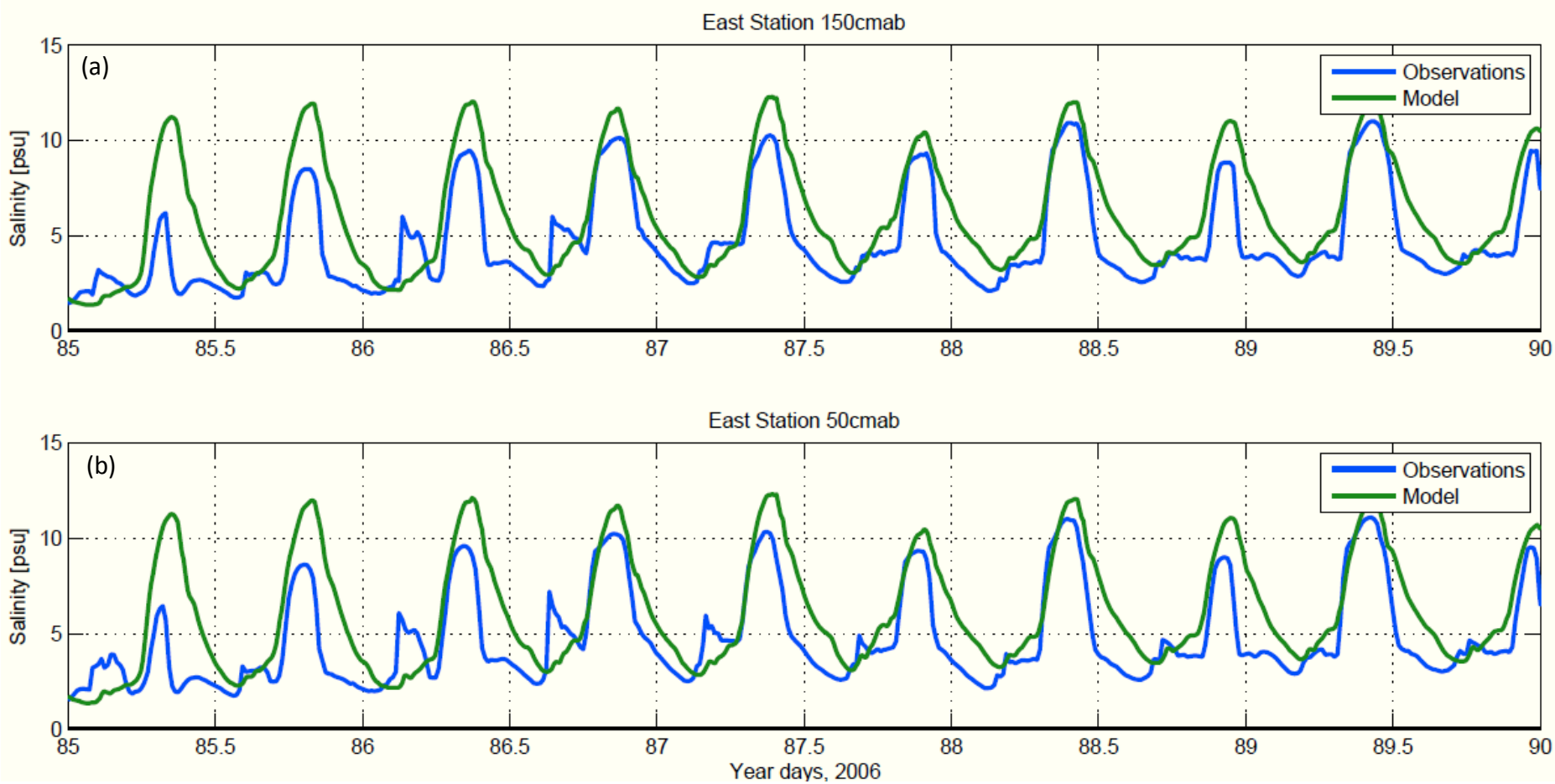

Figure 12: Comparison of modeled and predicted salinity at the "East" station at elevations of 150 cm above the bed (a) and 50 cm above the bed (b). The magnitude and phase of tidal variations in salinity is accurately modeled, including both the maximum and minimum values within the tidal cycle. The only feature not accurately reflected in the simulations is the abrupt decrease in salinity that occurs on each ebb tide. No calibration of these results have been pursued at this point, other than to provide a careful and complete accounting of freshwater sources throughout South Bay.

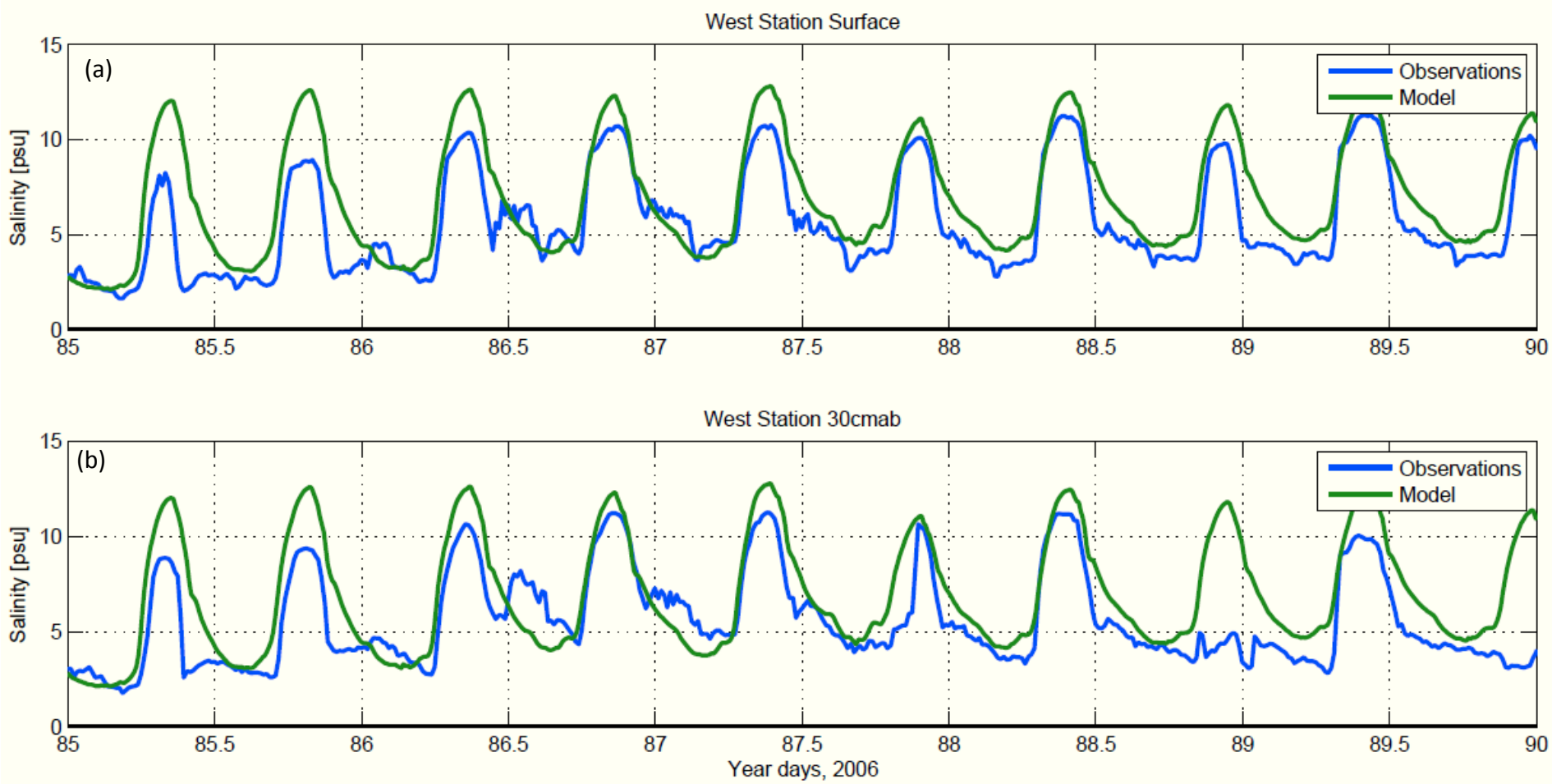

Figure 13: Comparison of modeled and predicted salinity at the "West" station at the surface (a) and 30 cm above the bed (b). The magnitude and phase of tidal variations in salinity is accurately modeled, including both the maximum and minimum values within the tidal cycle. Agreement at both the surface and the bottom indicates that vertical stratification is being accurately modeled in addition to the local salinities. No calibration of these results have been pursued at this point, other than to provide a careful and complete accounting of freshwater sources throughout South Bay.

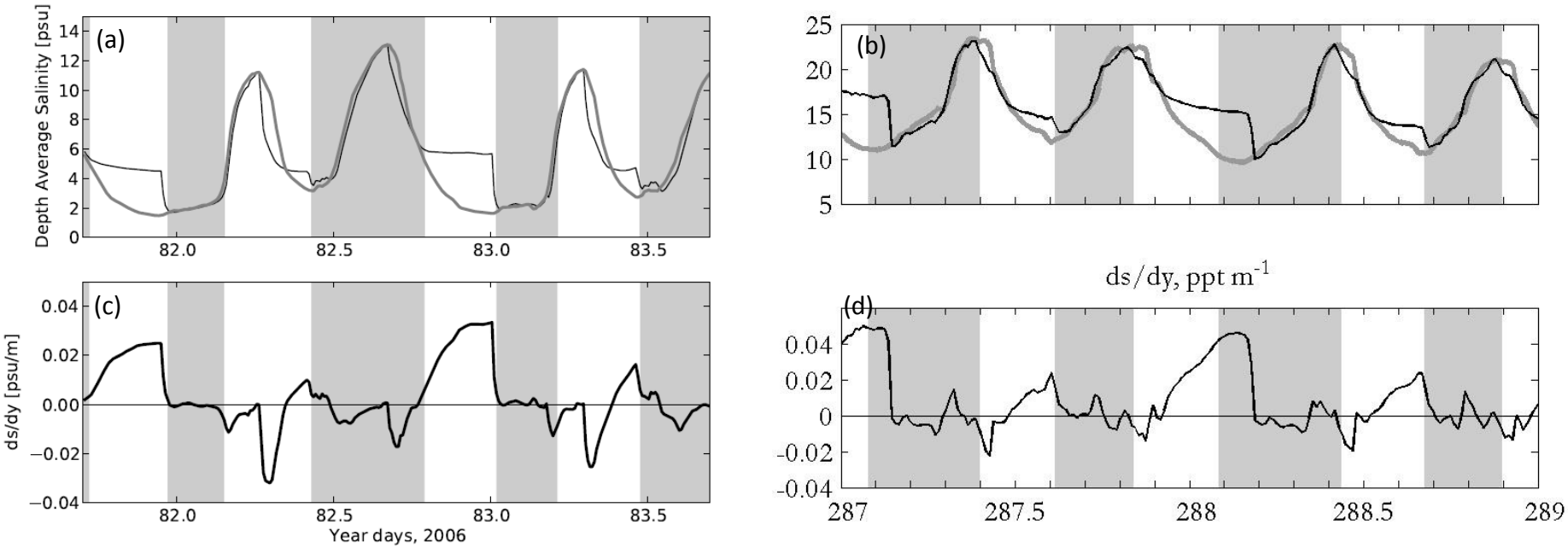

Figure 14: Comparison of modeled and predicted salinity differences between the channel center and the Pond breaches. Model results are in (a) and (c); observations are in (b) and (d). Note that these observations were from a different period than the simulations, so the absolute value of the salinity is not consistent between the model and observations; we focus here on the differences. The top panels ((a) and (b)) show the salinity in the center of the channel (light line) and adjacent to the breach (dark line). In both the model and the observations, the breach station (see Figure 15 for station location) has a period of constant salinity on each ebb tide, representing mixing in the interior of the ponds. A more sensitive comparison is shown in the lower panels ((c) and (d)), which is the inferred lateral salinity gradient. Here, although the phasing is slightly different in the model from the observations, the overall variability is very similar between the model and observation.

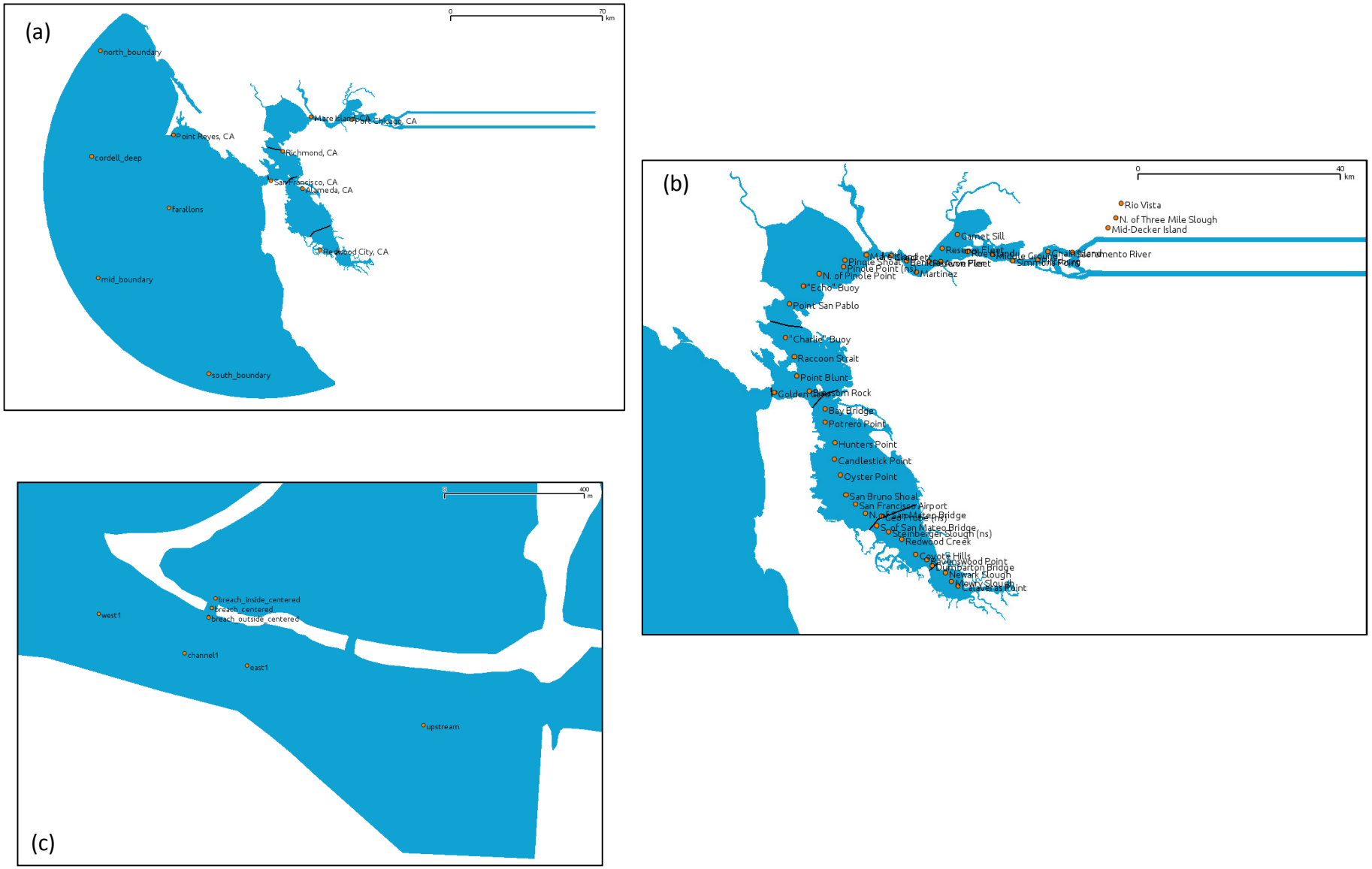

Figure 15: Summary of data output locations in addition to those shown in Figure 1. (a) NOAA stations for tidal stage comparisons; (b) USGS Polaris cruise stations sampled monthly; and (c) Island Pond stations, including breach stations shown in Figure 14.